encit 2020

ABCM Associação Brasileira de Engenharia e Ciências Mecânicas

18th Brazilian Congress of Thermal Sciences and Engineering
November 16–20, 2020 (Online)

ENC-2020-0163
PARTICLE SETTLING IN A THIXOTROPIC FLUID USING LATTICE BOLTZMANN METHOD

Marco A. Ferrari
Alan Lugarini
Admilson T. Franco
Research Center for Rheology and Non-Newtonian Fluids (CERNN), Universidade Tecnológica Federal do Paraná (UTFPR)
Deputado Heitor Alencar Furtado Street, 5000, 81290-000, Curitiba - PR, Brazil
marcoferrari@alunos.utfpr.edu.br, alansouza@utfpr.edu.br, admilson@utfpr.edu.br

Abstract. *Settling phenomenon is present in several industrial activities, such as in cuttings transport and vertical gravel pack in oil wellbores, and sedimentation of weighting agent in a heavy mixture. In particular, for the oil and gas industry, knowing the cuttings settling velocity in drilling mud is important since in some cases is necessary to determine the cuttings build-up rate at the bottom of the well. The drilling fluids often exhibit a property denominated thixotropy, or time-depend rheology, which is manifested by the mud's gelification and consequent reduction of the terminal velocity of the particle. In the present work a direct numerical simulation (DNS) using the coupling of the lattice Boltzmann method (LBM), extended to accommodate a thixotropic fluid model based in a structural parameter, and the immersed boundary method (IBM) are used to understand how the particle settling velocity changes with the rheological parameters. Considering that fluid starts to age as soon as the particle starts to settle, the velocity reaches a peak value and posteriorly slows down until it reaches a steady-state, sometimes reaching velocities below 10% of an unstructured fluid.*

Keywords: *Thixotropy, Particle Settling, Lattice Boltzmann Method, Immersed Boundary Method*

1. INTRODUCTION

During the wellbore drilling operation, cuttings are removed from the borehole by drilling fluid. When the circulation stops, the cuttings that are still in transport will settle towards the bottom. Field engineers in order to retard the settling rate of these particles use fluids which exhibit time-depend properties (thixotropy) that increase the viscosity over time when shear is removed, which consequently reduces the cuttings settling velocity.

Currently, the process to determine settling rate cuttings consists of correlations that depend on the fluid's rheology, particle size, and density ratio (Eustes, 2011). However, most of these correlations are for certain fluid models (Newtonians, Power-law, Bingham) and do not represent the temporal characteristics existing in a thixotropic fluid. Some studies (Ferroir *et al.*, 2004)(Moseley *et al.*, 2019) have analyzed the settling of spherical particles in thixotropic fluids proposing correlations for terminal velocity. In these studies, the Reynolds number range was restricted to the Stokes regime, however, the cuttings in the drilling column can reach Reynolds numbers in the order of 10^3, hence there is demand for terminal velocity data in a broader Reynolds number range.

The use of experimental data is ideal to determine new correlations of the terminal velocity, but experiments usually take a long time and the costs are relatively high. Because of this, we chose a numerical approach to obtain the necessary data. Among the various numerical methods to solve fluid flows, there is the lattice Boltzmann method (LBM). This method solve the flow in the mesoscopic scale and presents efficient parallelism when used in computer clusters, resulting in fast simulation speeds (Han *et al.*, 2018).

The addition of a settling body adds another level of complexity to the method. Numerical methods were created to add immersed bodies in the LBM. Among them, the immersed boundary method proposed by (Peskin, 1972) and adapted for the LBM by (Feng and Michaelides, 2004) stands out. In this method, Lagrangian nodes create a body force in the fluid, causing the same effect of a physical wall would create.

Thixotropy models can be divided into three categories (Barnes, 1997): phenomenological, direct, and indirect microstructural. In the later, a structural parameter is used to access the structuring level of the fluid between fully unstructured and structured. In this work, the LBM convection-diffusion equation is used with the transport of the structural parameter which will model the thixotropic behavior of a drilling fluid. This results in two mesoscopic equations being solved in parallel. Also, it will be analyzed the effect of the fluid parameters in the transient behavior of a spherical particle outside of the Stokes' regime starting from rest in a thixotropic fluid.

2. MATHEMATICAL MODEL

The lattice Boltzmann method solves the fluid flow in the mesoscopic scale, an intermediate step between the microscopic, ruled by inter-molecular collisions, and macroscopic scale, governed by the Navier-Stokes equation (Guo and Shu, 2013). On this scale, the temporal evolution of particle groups can be expressed by the Boltzmann equation. The lattice Boltzmann method is based on the phase-space discretization of the Boltzmann equation. One of the forms to discretization is the regularized version using the BGK collision operator proposed by Latt and Chopard (2006):

$$\bar{f}_i\left(\boldsymbol{x}+c_i\Delta t, t+\Delta t\right)=\left(1-\frac{1}{\bar{\tau}}\right)f_i^{reg}\left(\boldsymbol{x},t\right)+\frac{1}{\bar{\tau}}f_i^{eq}\left(\boldsymbol{x},t\right)+\left(1-\frac{1}{2\bar{\tau}}\right)F_i\left(\boldsymbol{x},t\right)\Delta t, \tag{1}$$

where f_i is the particle distribution function in the i direction, $\boldsymbol{c}_i$ is the velocity vector in the i direction, $\bar{\tau}$ is the relaxation time, F_i is the body force acting in the fluid, Δt is the timestep, f_i^{reg} is the regularized distribution function:

$$f_i^{reg}=f_i^{eq}+f_i^{(1)} \tag{2}$$

where $f_i^{(1)}$ is the second term of expansion $f_i=f_i^{(0)}+\epsilon f_i^{(1)}+\epsilon^2 f_i^{(2)}+\ldots$ from the Chapman-Enskog expansion (Buick and Greated, 2000). f_i^{eq} is the equilibrium distribution function defined as (Philippi *et al.*, 2006):

$$f_i^{eq}=w_i\rho\left[1+\frac{c_{i\alpha}u_\alpha}{c_s^2}+\frac{u_\alpha u_\beta\left(c_{i\alpha}c_{i\beta}-c_s^2\delta_{\alpha\beta}\right)}{2c_s^4}\right] \tag{3}$$

where w_i is the weight, ρ is the fluid density, u is the fluid velocity in the α direction, and c_s is the speed of the sound. The force term is defined as (Guo *et al.*, 2002):

$$F_i=w_i\left[\frac{c_{i\alpha}}{c_s^2}+\frac{\left(c_{i\alpha}c_{i\beta}-c_s^2\delta_{\alpha\beta}\right)u_\beta}{c_s^4}\right]F_\alpha \tag{4}$$

where F_α is the force components in the cartesian coordinate system.

In the LBM, velocity-space is divided into lattices, denominated velocity set. In this work, the velocity set D3Q19 is utilized, it is three-dimensional with 19 possible directions, index i of the previous equations. The values for c_i and the respectively w_i in the D3Q19 velocity set are:

$$c_i=\begin{cases}(0,0,0), & i=0 \qquad w_i=1/3\\ (\pm1,0,0),(0,\pm1,0),(0,0,\pm1), & i=1,...,6 \qquad w_i=1/18\\ (\pm1,\pm1,0),(\pm1,0,\pm1),(0,\pm1,\pm1), & i=7,...,19 \qquad w_i=1/36\end{cases} \tag{5}$$

The fluid flow properties can be determined based on the momentum of the particle distribution function on the velocity space (Silva and Semiao, 2012):

$$\rho=\Pi_0=\sum_i\bar{f}_i+\frac{\Delta t}{2}\sum_i F_i \tag{6a}$$

$$\rho u_\alpha=\Pi_\alpha=\sum_i\bar{f}_i c_{i\alpha}+\frac{\Delta t}{2}\sum_i F_i c_{i\alpha} \tag{6b}$$

$$\Pi_{\alpha\beta}=\left(1-\frac{\Delta t}{2\bar{\tau}}\right)\sum_i\bar{f}_i c_{i\alpha}c_{i\beta}+\frac{\Delta t}{2\bar{\tau}}\sum_i\bar{f}_i^{eq}c_{i\alpha}c_{i\beta}+\frac{\Delta t}{2}\left(1-\frac{\Delta t}{2\bar{\tau}}\right)\sum_i F_i c_{i\alpha}c_{i\beta} \tag{6c}$$

Through a Chapman–Enskog expansion (Lugarini *et al.*, 2020) the fluid apparent viscosity (η) is correlated with the relaxation time as:

$$\bar{\tau}=\frac{\eta}{\rho c_s^2}+\frac{\Delta t}{2}. \tag{7}$$

To model the thixotropic behavior of the fluid, an indirect microstructural model is utilized. The structural parameter needs to be transport through the fluid, for that the convection–diffusion equation is utilized:

$$\frac{\partial\lambda}{\partial t}+\frac{\partial\left(u_i\lambda\right)}{\partial x_i}=\frac{\partial}{\partial x_i}\left(D\frac{\partial\lambda}{\partial x_i}\right)+q \tag{8}$$

where D is diffusivity factor and q is the source term. This equation can be converted to mesoscopic scale (Chopard *et al.*, 2009)(Seta, 2013):

$$g_i\left(\boldsymbol{x}+c_i\Delta t, t+\Delta t\right)=\left(1-\frac{1}{\bar{\tau}_g}\right)g_i\left(\boldsymbol{x},t\right)+\frac{1}{\bar{\tau}_g}g_i^{eq}\left(\boldsymbol{x},t\right)+\left(1-\frac{1}{2\tau_g}\right)w_i q\left(\boldsymbol{x},t\right), \tag{9}$$

$$g_i^{eq}=w_i\lambda\left[1+\frac{c_{i\alpha}u_\alpha}{c_s^2}+\frac{u_\alpha u_\beta\left(c_{i\alpha}c_{i\beta}-c_s^2\delta_{\alpha\beta}\right)}{2c_s^4}\right] \tag{10}$$

$$\lambda=\sum_i g_i+\left(1-\frac{1}{2\tau_g}\right)\frac{w_i\Delta t}{2}q \tag{11}$$

$$\bar{\tau}_g=\frac{D}{c_s^2}+\frac{\Delta t}{2} \tag{12}$$

where g_i is the distribution function for the structural parameter, $\bar{\tau}_g$ is the relaxation time associated with diffusion of the structural parameter, and g_i^{eq} is the equilibrium distribution function. On this work is adopted the model utilized by Ferroir *et al.* (2004):

$$\boldsymbol{\tau}=\eta(\lambda)\dot{\boldsymbol{\gamma}}, \tag{13a}$$

$$\eta(\lambda)=\eta_\infty\left(1+\alpha\lambda\right), \tag{13b}$$

$$\frac{\partial\lambda}{\partial t}+u_i\frac{\partial\lambda}{\partial x_i}=-k_1\lambda\dot{\gamma}+k_2(1-\lambda)=q, \tag{13c}$$

where α_∞ is the apparent viscosity for a totally unstructured fluid, $(1+\theta)$ is viscosity ratio between a structured and unstructured fluid, $\dot{\gamma}$ is the strain-rate magnitude, k_1 is the breakdown constant, and k_2 is the build up constant. In order to eliminate the inherent diffusivity, $\bar{\tau}_g$ needs to be approximately 0.5.

The immersed Boundary method for LBM proposed by Feng and Michaelides (2004) is utilized for model the immersed particle. On this method, Lagrangian nodes are placed over the Eulerian lattices of the LBM. These nodes exert a force over the neighbor lattices:

$$\boldsymbol{F}^E=\sum_L \boldsymbol{F}^L\delta\left(\boldsymbol{x}-\boldsymbol{X}\right)\Delta S, \tag{14}$$

where $\boldsymbol{F}^E$ is the force in the Eulerian node, $\boldsymbol{F}^L$ is the force in the Lagrangian node, ΔS is the surface area of the Lagrangian node, and $\delta\left(\boldsymbol{x}-\boldsymbol{X}\right)$ is the discrete Dirac's delta between a Eulerian lattice $\boldsymbol{x}$ and a Lagragian node $\boldsymbol{X}$ proposed by Peskin (2002):

$$\delta\left(\boldsymbol{x}-\boldsymbol{X}\left(s,t\right)\right)=\frac{1}{h^3}\phi\left(\frac{x-X}{h}\right)\phi\left(\frac{y-Y}{h}\right)\phi\left(\frac{z-Z}{h}\right) \tag{15}$$

where h is the lattice size and ϕ is defined as:

$$\phi_4\left(r\right)=\begin{cases}\frac{1}{8}\left(3-2|r|+\sqrt{1+4|r|-4|r|^2}\right) & 0\leq|r|\leq h\\ \frac{1}{8}\left(5-2|r|-\sqrt{-7+12|r|-4|r|^2}\right) & h<|r|\leq 2h\\ 0 & 2h<|r|\end{cases} \tag{16}$$

The force is used to update the Eulerian velocity. The no-slip condition between the lattices and the Lagrangian nodes must be satisfied, hence:

$$\boldsymbol{u}^L=\sum_E\left[\boldsymbol{u}^{E,noF}+\frac{\Delta t}{2\rho}\boldsymbol{F}^E\right]\delta\left(\boldsymbol{x}-\boldsymbol{X}\right)h^3, \tag{17}$$

where $\boldsymbol{u}^L$ is the velocity of the Lagrangian node, and $\boldsymbol{u}^{E,noF}$ is the velocity in the Eulerian lattice without the force term. The equation system formed by Eq. (14) and Eq. (17) is then solved by the iterative method proposed by Dash *et al.* (2014). To account for the internal fluid mass the rigid body approximation of Feng and Michaelides (2009) is utilized:

$$\boldsymbol{U}_p^{t+1}=\left(1+\frac{\rho_f}{\rho_p}\right)\boldsymbol{U}_p^t-\frac{\rho_f}{\rho_p}\boldsymbol{U}_p^{t-1}+\frac{1}{m_p}\left[-\sum_{L_p}\boldsymbol{F}^L h\Delta S+\left(m_p-m_f\right)\boldsymbol{g}\right]\Delta t, \tag{18}$$

$$\boldsymbol{X}_p^{t+1}=\boldsymbol{X}_p^t+\frac{\boldsymbol{U}_p^{t+1}+\boldsymbol{U}_p^t}{2}\Delta t, \tag{19}$$

where $\boldsymbol{U_p^t}$ is the particle velocity in the time t, ρ_f is the fluid density, ρ_p the particle density, m_p the particle mass, m_f the internal fluid mass, $\boldsymbol{g}$ is the gravitational acceleration, and $\boldsymbol{X_p^t}$ is the particle position in the time t. The particle angular velocity is obtained as:

$$\boldsymbol{\omega}_p^{t+1} = \left(1 + \frac{\rho_f}{\rho_p}\right)\boldsymbol{\omega}_p^t - \frac{\rho_f}{\rho_p}\boldsymbol{\omega}_p^{t-1} + \boldsymbol{I}_p^{-1}\left[-\sum_{L_p}\left(\boldsymbol{X}^t - \boldsymbol{X}_p^t\right) \times \boldsymbol{F}^L h\Delta S\right]\Delta t, \tag{20}$$

where $\boldsymbol{\omega}_p^t$ is the particle angular velocity in the time t, $\boldsymbol{I}$ the inertia tensor of the particle, and $\boldsymbol{X} - \boldsymbol{X}_p$ is the vector between the particle's center of mass and the Lagrangian nodes that are part of the particle.

In summary, the lattice Boltzmann method is utilized to solve both the Navier-Stokes equations and the structural parameter, responsible for the thixotropy, with the convection–diffusion equation modeled as another set of LBM populations. Finally, the immersed boundary method is used to solve the particle dynamics.

3. VALIDATION CASES

3.1 Settling in a Newtonian Fluid

The first test assesses the capability of the numerical methodology to represent the particle settling phenomenon. The model is based on the experiments of Ten Cate *et al.* (2002), where a spherical particle with diameter of $15\,\mathrm{mm}$ have its center $127.5\,\mathrm{mm}$ from the bottom of a rectangular container with dimensions of $100\,\mathrm{mm} \times 100\,\mathrm{mm} \times 160\,\mathrm{mm}$. Table 1 shows the four cases analyzed and its properties. The time-step values are for mesh size of $h = 0.66\,\mathrm{mm}$, given that on this refinement level it was obtained mesh independence. The ratio between the distance of the Langrangian nodes that build the spherical particle and the Eulerian lattice was approximately 1. Figure 1 brings the results for the particle velocity as

Table 1. Fluid properties for each test case as well as the simulation relaxation time and time-step.

Case	$Re_D = \rho_f U D/\mu_f$	ρ_f [kg m^{-3}]	μ_f[Pa s]	τ	Δt [s]
1	1.5	970	0.373	0.90	1.54×10^{-4}
2	4.1	965	0.212	0.90	2.70×10^{-4}
3	11.6	962	0.113	0.80	3.78×10^{-4}
4	31.9	960	0.058	0.65	3.68×10^{-4}

well as the trajectory. The results show accordance with the experimental results of Ten Cate *et al.* (2002). The errors presented in last case can be associated with the drag coefficient being depend of the kernel utilized and the lattice velocity (Fučík *et al.*, 2019). Overall the results are satisfactory regarding the implementation of the immersed boundary method and internal mass dynamics.

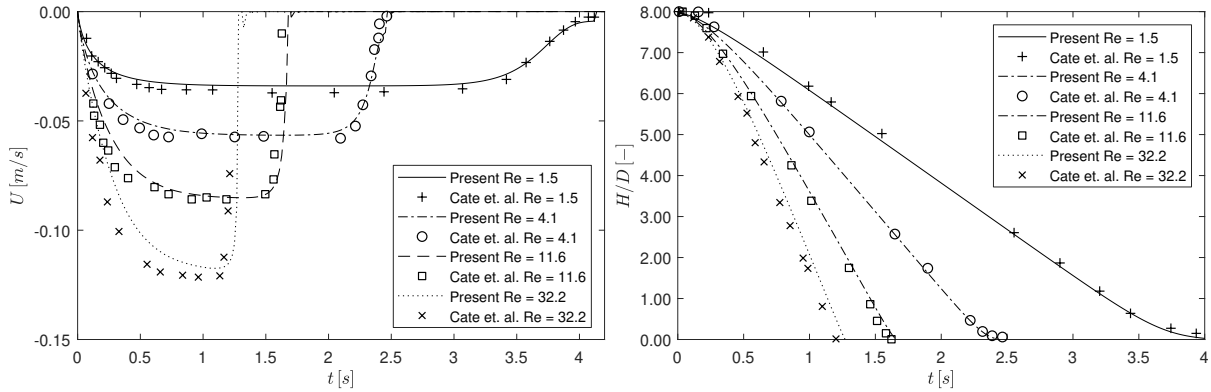

Figure 1. Comparison between numerical results of the velocity and trajectory and experimental data (Ten Cate *et al.*, 2002) of a spherical particle settling in a Newtonian fluid.

3.2 Thixotropic Hagen–Poiseuille Flow

The second problem used to validate the numeric model is the Hagen-Poiseuille flow between two infinite parallel plates with a thixotropic fluid. Initially, an unstructured fluid ($\lambda = 0$) is at rest between two plates, with a distance H separating them. A body force $\vec{F}$ is then applied to the fluid with a direction parallel to the plates. After a period, the flow

reaches the steady state. The mesh independence test was performed with $\tau_g = 0.5003$, $k_1 = 1$, $k_2 = 10^{-4}$, $\eta_\infty = 0.01$, $\alpha = 40$, and $\tau = 0.65$. The results for the quadratic error are presented in the Tab. 2 with the respective number of time-steps.

Table 2. Dimensional parameters and L_2 errors for thixotropic Hagen-Poiseuille flow.

$N \times N \times L$	Time Steps	$L_2(\lambda)$
$7 \times 7 \times 4$	7800	1.38×10^{-1}
$12 \times 12 \times 4$	31 250	2.60×10^{-2}
$25 \times 25 \times 8$	125 000	3.60×10^{-3}
$51 \times 51 \times 16$	500 000	8.62×10^{-4}
$102 \times 102 \times 32$	2 000 000	3.69×10^{-5}

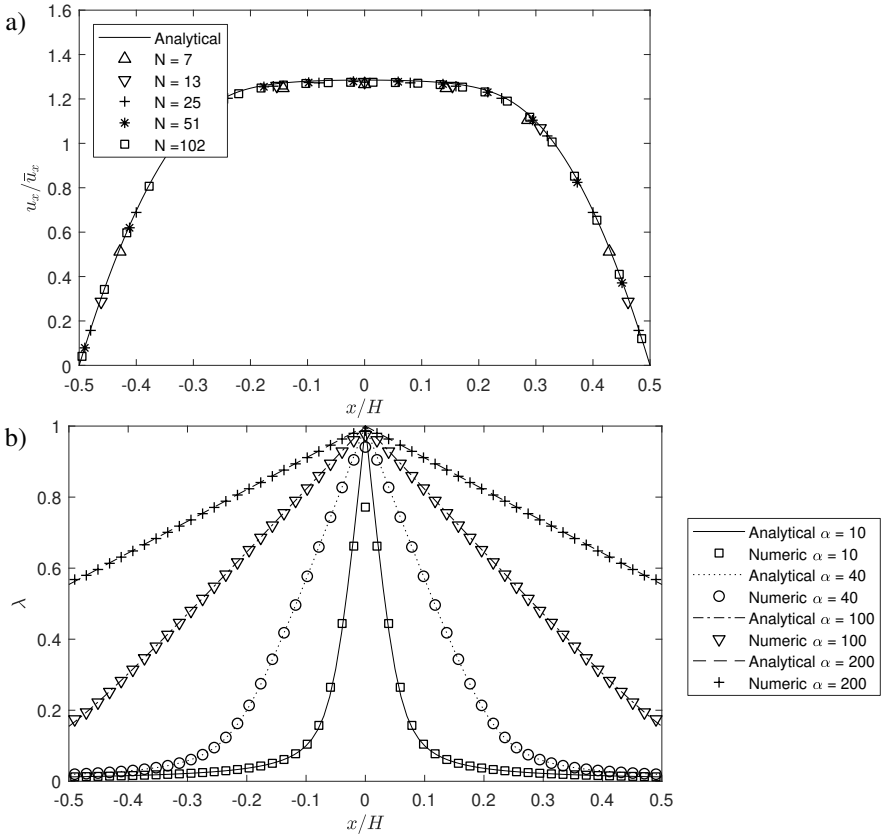

Figure 2. Comparison between numerical and analytical results for a thixotropic Hagen–Poiseuille between two parallel plates. a) Velocity profile as function of lattices. b) Structural parameter profile for different viscosity ratios.

The quadratic error for the structural parameter in $N = 7$ was 1.4×10^{-1} and reduced approximately with a second order until $N = 102$ where the error was 8.6×10^{-5}. A justification for this error is that with lower mesh resolution, there isn't enough resolution to correctly calculate the gradient of λ in the channel. This gradient can be perceived in Fig. 2.b, where the profile of λ across the channel for different values of α is shown when a constant force is applied.

With the increase of α the fluid has a higher maximum viscosity, the strain-rate magnitude at the walls decreases, causing an increase in the steady-state value of λ. In the channel center, the strain-rate is zero, consequently, the value for the structural parameter will be 1 in the steady-state. In summary, the model can capture the peculiarities of the thixotropic model and the errors on both velocity and lambda fields decay quadratically with the spatial resolution.

4. SETTLING IN A THIXOTROPIC FLUID

The problem is defined as follows. A spherical particle with diameter D is initially at rest in a rectangular tank containing a thixotropic fluid. The tank has dimensions of $6.7D \times 6.7D \times 26.7D$, with the particle center positioned $24.5D$ from the tank's bottom. The particle is composed of 1158 Lagrangian nodes with a distance between them equal to 1 and the particle/fluid density ratio is $\rho_p/\rho_f = 1.16$. The fluid is initially completely unstructured ($\lambda_0 = 0$) and presents

a viscosity $\eta_\infty/\sqrt{gD^3} = 0.0163$. As soon as the simulation starts, the particle settles while the fluid ages. The effect of thixotropic properties on the particle's trajectory and terminal velocity are of interest. Viscosity ratios of $\alpha = 0$, 1, 3, 10, and 30 and build up parameters of $k_2/\sqrt{g/D} = 2.6 \times 10^{-3}$, 8.6×10^{-3}, 2.6×10^{-2}, and 8.6×10^{-2}. The breakdown rate is kept constant at $k_1 = 1$.

The first analysis focus on the effect of the build-up. The particle velocity over time is shown in Fig. 3. Initially, the

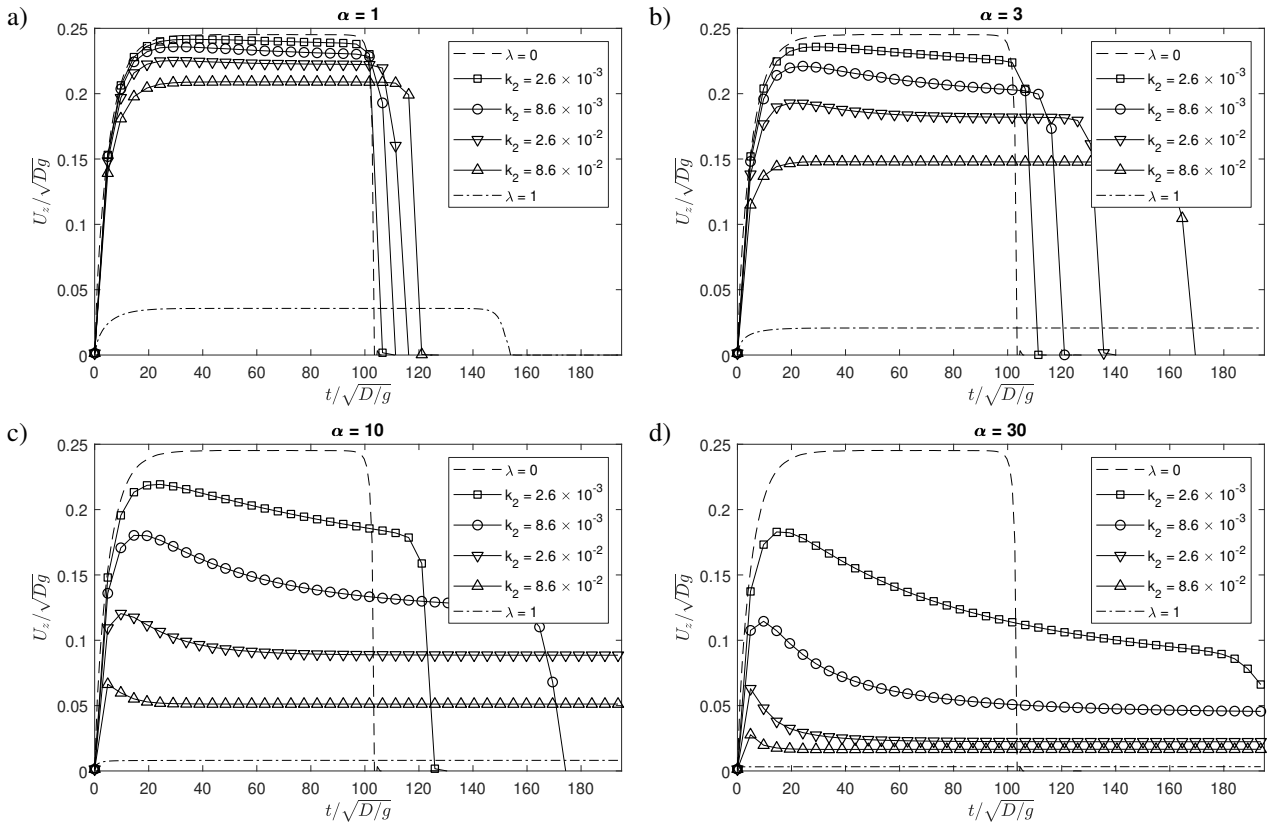

Figure 3. Settling velocity of a spherical particle as function of the breakdown/build-up rates. Dashed lines represent a velocity for a Newtonian fluid with viscosity equivalent to $\lambda = 0$ and $\lambda = 1$. a) $\alpha = 1$, b) $\alpha = 3$, c) $\alpha = 10$, d) $\alpha = 30$.

particle abruptly accelerates, due to the reduced viscosity of the unstructured fluid and the gravity force. After a period, the particle velocity reduces, this is a consequence of the aging process in the fluid that exists below, which increased the its viscosity. If enough time is passed, the particle will reach a terminal velocity, which happens when the rate of breakdown and build-up of the fluid structure is the same. As expected the particle settling velocity in a thixotropic fluid is between the upper and lower limit imposed by the Newtonian equivalents, represented by the dashed lines $\lambda = 0$ and $\lambda = 1$ respectively. Another aspect is that increasing the build-up rate parameter, the velocity of the particle approaches the equivalent velocity as if was settling in a fluid with higher viscosity. This occurs because recovers faster when broke by the settling particle, this causes a higher level of structured material around the body and consequently a higher viscosity. This effect can be seen in Fig. 4, where is shown the structural parameter value for different levels of build-up rate. When the particle is settling, the fluid in the fore section needs to be displaced, causing the material to breakdown. Another aspect that can be perceived is the formation of a wake of reduced viscosity behind the particle. This wake is formed by the passage of the particle in the fluid, which breaks the structures that may exist. The wake is consequently longer for a fluid which has lower build-up rate, Fig. 4.a, when compared to a fluid with a higher build up rate, Fig. 4.c, because the material broke less due the reduced particle velocity and also structure faster. When the build-up parameter is low, the particle will take a longer time to reach a steady-state situation, and in some of the simulated cases the particle collided with the bottom of the domain, indicated by the sudden reduction in the velocity, as shown in the Fig. 3, before terminal velocity be obtained. Because the fluid needs a longer time to structured, it is expected for the particle also take some time to reach its terminal velocity since the true steady-state will be only achieved when the $\lambda_\infty = 1$.

Shifting the view of the results to a constant build-up rate and varying the viscosity ratio, as shown in Fig. 5, some important considerations can be made. First, the time for steady-state is strongly correlate with the build-up rate and not with the viscosity ratio. This can be clearly seen in the Fig. 3.c and Fig. 3.d, where the time to reach the steady-state is approximately 60 and 20 respectively. This time correspond to a state where the value of the structural parameter in undisturbed fluid recovers to a value superior to 0.95. For lower build-up rates the steady-state is not possible verify this

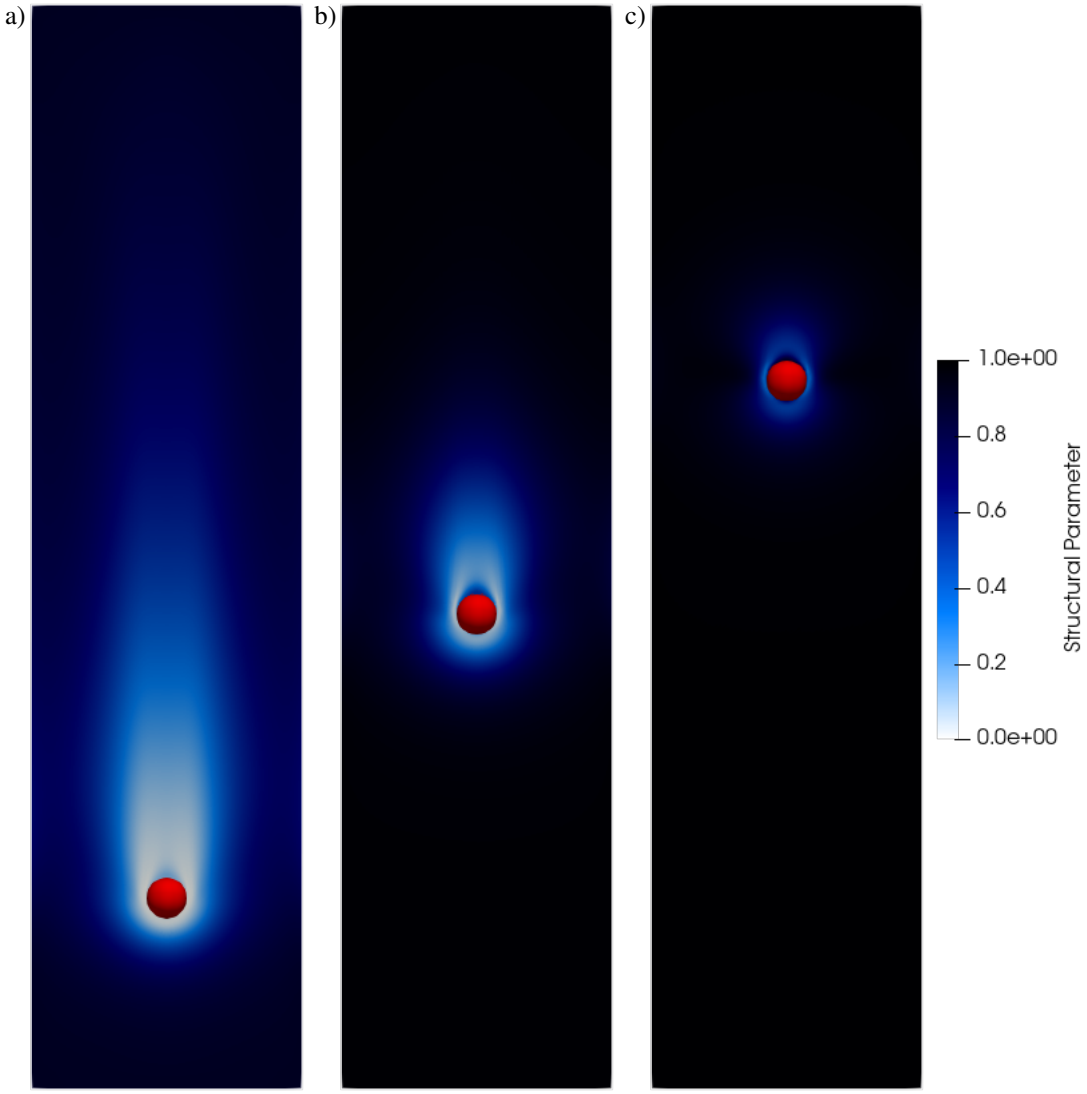

Figure 4. Structural parameter values of the middle XZ plane for $\alpha = 10$, showing the breakdown wake formed by settling sphere in $t/\sqrt{D/g} = 135$. a) $k_2/\sqrt{g/D} = 8.6 \times 10^{-3}$, b) $k_2/\sqrt{g/D} = 2.6 \times 10^{-2}$, c) $k_2/\sqrt{g/D} = 8.6 \times 10^{-2}$.

conclusion due the particle reaching the end of the domain.

The ratio of the overshoot velocity versus the terminal velocity increases with the viscosity ratio. For $\alpha = 1$, no overshoot was visualized, but when the viscosity ratio increases to $\alpha = 30$ the maximum particle velocity in some case was 2.5 times the value of the terminal velocity. This is important because the average particle settling velocity will depend not only of the rheological properties of the fluid but also the length which the particle will travel.

5. CONCLUSION

In this study, the convection-diffusion equation in the mesoscopic scale was extended to be used with a thixotropic fluid and then applied in the settling of a spherical particle in an unstructured fluid. The source term was used to represent the breakdown and build-up of a thixotropic fluid. As the particle settle and the fluid ages, the particle reaches its peak velocity. After that, the aging process slows down the particle until it reaches a terminal velocity, which for some cases was less than half of the maximum velocity. The terminal velocity is intrinsically related with both the viscosity ratio and the rates on which the fluid breaks and builds-up. This is because as the build-up rate increases the particle weight is not capable to break down the fluid with the same efficiency, causing a higher value for the steady-state structural parameter and consequently the terminal velocity attained by the particle decreases. Meanwhile the time for steady state is strongly related with the build-up rate of the fluid and not with viscosity. Therefore in order to determine the average rate which cuttings will settle in a thixotropic fluid is not only important know the fluid properties but is also important know the length which the which this particles will travel.

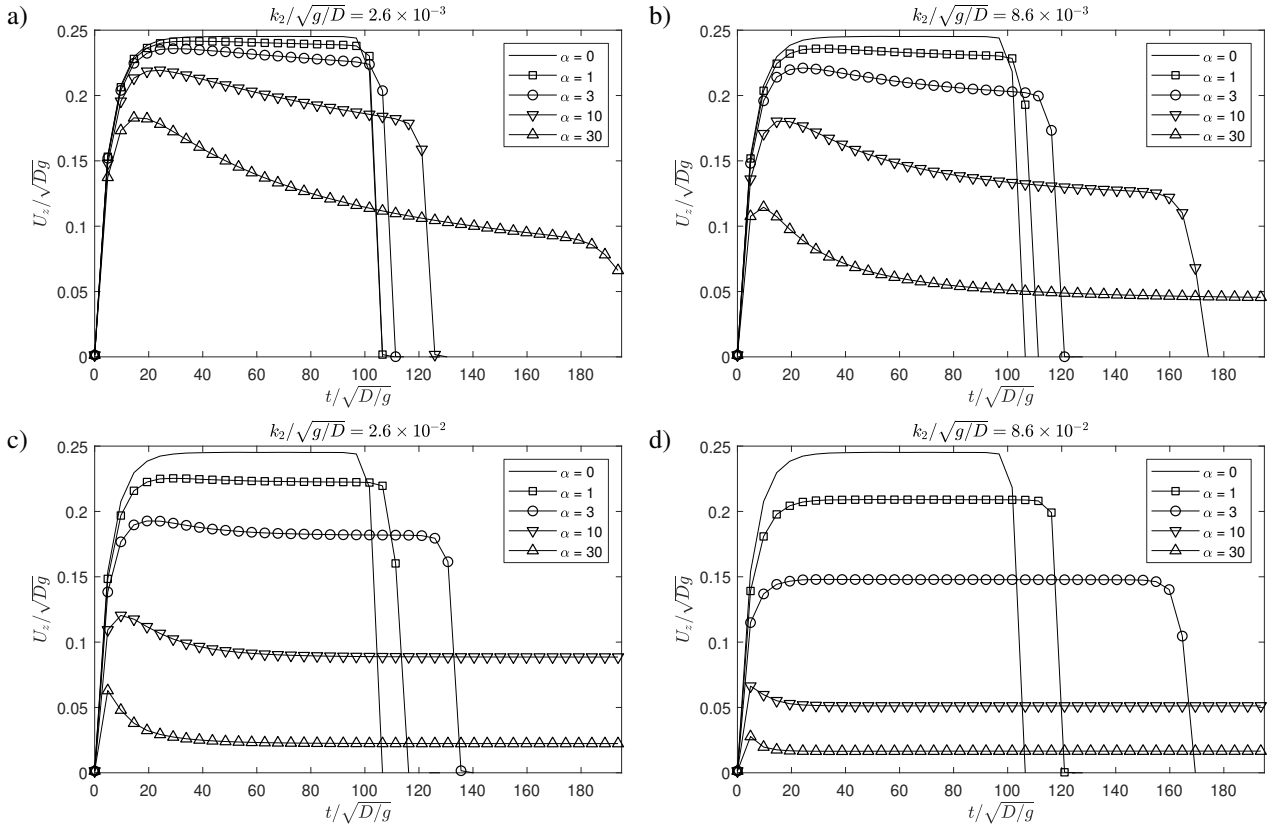

Figure 5. Settling velocity of a spherical particle as function of viscosity ratio in different breakdown/build-up ratios. a) $k_2/\sqrt{g/D} = 2.6 \times 10^{-3}$, b) $k_2/\sqrt{g/D} = 8.6 \times 10^{-3}$, c) $k_2/\sqrt{g/D} = 2.6 \times 10^{-2}$, d) $k_2/\sqrt{g/D} = 8.6 \times 10^{-2}$.

6. ACKNOWLEDGEMENTS

This study was financed in part by the Coordenação de Aperfeiçoamento de Pessoal de Nível Superior - Brasil (CAPES) - Finance Code 001.

7. REFERENCES

Barnes, H.A., 1997. "Thixotropy—a review". *Journal of Non-Newtonian Fluid Mechanics*, Vol. 70, No. 1-2, pp. 1–33.

Buick, J.M. and Greated, C.A., 2000. "Gravity in a lattice Boltzmann model". *Physical Review E*, Vol. 61, No. 5, pp. 5307–5320.

Chopard, B., Falcone, J.L. and Latt, J., 2009. "The lattice Boltzmann advection-diffusion model revisited". *European Physical Journal: Special Topics*, Vol. 171, No. 1, pp. 245–249.

Dash, S., Lee, T., Lim, T. and Huang, H., 2014. "A flexible forcing three dimension IB–LBM scheme for flow past stationary and moving spheres". *Computers & Fluids*, Vol. 95, pp. 159–170.

Eustes, A., 2011. *Drilling Fluids*, Vol. 12. 1st edition.

Feng, Z.G. and Michaelides, E.E., 2004. "The immersed boundary-lattice Boltzmann method for solving fluid–particles interaction problems". *Journal of Computational Physics*, Vol. 195, No. 2, pp. 602–628.

Feng, Z.G. and Michaelides, E.E., 2009. "Robust treatment of no-slip boundary condition and velocity updating for the lattice-Boltzmann simulation of particulate flows". *Computers & Fluids*, Vol. 38, No. 2, pp. 370–381.

Ferroir, T., Huynh, H.T., Chateau, X. and Coussot, P., 2004. "Motion of a solid object through a pasty (thixotropic) fluid". *Physics of Fluids*, Vol. 16, No. 3, pp. 594–601.

Fučík, R., Eichler, P., Straka, R., Pauš, P., Klinkovský, J. and Oberhuber, T., 2019. "On optimal node spacing for immersed boundary–lattice Boltzmann method in 2D and 3D". *Computers & Mathematics with Applications*, Vol. 77, No. 4, pp. 1144–1162.

Guo, Z. and Shu, C., 2013. *Lattice Boltzmann Method and Its Applications in Engineering*, Vol. 3 of *Advances in Computational Fluid Dynamics*. WORLD SCIENTIFIC.

Guo, Z., Zheng, C. and Shi, B., 2002. "Discrete lattice effects on the forcing term in the lattice Boltzmann method". *Physical Review E*, Vol. 65, No. 4, p. 046308.

Han, M., Ooka, R. and Kikumoto, H., 2018. "Comparison of Lattice Boltzmann Method and Finite Volume Method

with Large Eddy Simulation in Isothermal Room Flow". In *Healthy, Intelligent and Resilient Buildings and Urban Environments*. International Association of Building Physics (IABP), Syracuse, New York, September 2018, pp. 1121–1126.

Latt, J. and Chopard, B., 2006. "Lattice Boltzmann method with regularized pre-collision distribution functions". *Mathematics and Computers in Simulation*, Vol. 72, No. 2-6, pp. 165–168.

Lugarini, A., Franco, A.T. and Philippi, P.C., 2020. "Lattice Boltzmann method for viscoplastic fluid flow based on regularization of ghost moments". *Journal of Non-Newtonian Fluid Mechanics*, p. 104413.

Moseley, K., Fairweather, M. and Harbottle, D., 2019. "Settling dynamics of two identical vertically aligned spheres in a thixotropic fluid". *Journal of Non-Newtonian Fluid Mechanics*, Vol. 271, No. June, p. 104146.

Peskin, C.S., 1972. "Flow patterns around heart valves: A numerical method". *Journal of Computational Physics*, Vol. 10, No. 2, pp. 252–271.

Peskin, C.S., 2002. "The immersed boundary method". *Acta Numerica*, Vol. 11, No. May 2019, pp. 479–517.

Philippi, P.C., Hegele, L.A., dos Santos, L.O.E. and Surmas, R., 2006. "From the continuous to the lattice Boltzmann equation: The discretization problem and thermal models". *Physical Review E*, Vol. 73, No. 5, p. 056702.

Seta, T., 2013. "Implicit temperature-correction-based immersed-boundary thermal lattice Boltzmann method for the simulation of natural convection". *Physical Review E - Statistical, Nonlinear, and Soft Matter Physics*, Vol. 87, No. 6, pp. 1–16.

Silva, G. and Semiao, V., 2012. "First-and second-order forcing expansions in a lattice Boltzmann method reproducing isothermal hydrodynamics in artificial compressibility form". *Journal of Fluid Mechanics*, Vol. 698, pp. 282–303.

Ten Cate, A., Nieuwstad, C.H., Derksen, J.J. and Van den Akker, H.E.A., 2002. "Particle imaging velocimetry experiments and lattice-Boltzmann simulations on a single sphere settling under gravity". *Physics of Fluids*, Vol. 14, No. 11, pp. 4012–4025.

8. RESPONSIBILITY NOTICE

The authors are solely responsible for the printed material included in this paper.